Large quantum rings in the v > 1 quantum Hall regime

2009 J. Phys.: Condens. Matter 21 025301

(http://iopscience.iop.org/0953-8984/21/2/025301)

J. Phys.: Condens. Matter **21** (2009) 025301 (5pp) doi:10.1088/0953-8984/21/2/025301

Large quantum rings in the $\nu > 1$ quantum Hall regime

E Räsänen[1,2,3,5] **and M Aichinger**[3,4]

[1] Institut für Theoretische Physik, Freie Universität Berlin, Arnimallee 14, D-14195 Berlin, Germany
[2] European Theoretical Spectroscopy Facility (ETSF)
[3] Institut für Theoretische Physik, Johannes Kepler Universität, A-4040 Linz, Austria
[4] MathConsult GmbH, Altenberger Strasse 69, A-4040 Linz, Austria

E-mail: erasanen@jyu.fi

Received 17 September 2008
Published 9 December 2008
Online at stacks.iop.org/JPhysCM/21/025301

Abstract
We study computationally the ground-state properties of large quantum rings in the filling-factor $\nu > 1$ quantum Hall regime. We show that the arrangement of electrons into different Landau levels leads to clear signatures in the total energies as a function of the magnetic field. In this context, we discuss possible approximations for the filling factor ν in the system. We are able to characterize integer-ν states in quantum rings in an analogy with conventional quantum Hall droplets. We also find a partially spin-polarized state between $\nu = 2$ and 3. Despite the specific topology of a quantum ring, this state is strikingly reminiscent of the recently found $\nu = 5/2$ state in a quantum dot.

(Some figures in this article are in colour only in the electronic version)

1. Introduction

Ever since the discovery of the Aharonov–Bohm (AB) effect, ring-shaped quantum systems have attracted lots of interest both theoretically and experimentally. The development of nanotechnology has rapidly led to a variety of techniques to fabricate quantum rings (QRs) [1–3]. The high tunability of the size and shape of QRs and the controllability of electronic states by external fields provides applications in the field of quantum information. For example, it was proposed very recently that laser-controlled single-electron semiconductor QRs could be used as qubit gates [4].

The single-electron states of QRs are periodic in the magnetic flux quantum $\Phi_0 = h/e$, whereas the electron–electron interactions have been found to lead to fractional AB oscillations [3, 5–7]. When the number of electrons increases above $N \sim 10$, the oscillations may become quasiperiodic due to the increasing degeneracy of the many-electron states. Furthermore, a realistic two-dimensional (2D) width of the QR, i.e., allowing the electrons to move in the radial direction, leads to the filling of several Landau levels and thus to additional complexity in the ground-state sequence as a function of the external magnetic field B [8]. Generally, however, both theory and Coulomb-blockade experiments on QRs [9] have shown the gradual depopulation of higher Landau levels when B is increased.

Changes in the ground state as a function of the magnetic field can be seen as kinks in the total energy $E(N)$, or pronouncedly in the chemical potentials, $\mu_N = E_N - E_{N-1}$, or in the magnetization defined at zero temperature as $M = -\partial E/\partial B$. In semiconductor quantum-dot (QD) studies [10], the features in $\mu(B)$ and $M(B)$ have been associated with the Landau-level filling factors $\nu_{\rm LL} = N/N_{\rm 0LL}$, where $N_{\rm 0LL}$ is the number of electrons in the lowest Landau level (0LL). At magnetic fields corresponding to integer $\nu_{\rm LL} \geqslant 1$, the energetics of QDs has been found to exhibit pronounced kinks [11, 12]. Recently, the fractional $\nu = 5/2$ state has also been characterized in large QDs [13, 14].

It is noteworthy that, in contrast to a uniform two-dimensional electron gas, there is no fully consistent way to define the filling factor in spatially restricted systems such as QRs and QDs. At large magnetic fields in the fractional $\nu < 1$ regime, the filling factor can be most conveniently estimated by applying the standard formula of the uniform quantum Hall system, i.e., $\nu_\Phi = N/N_\Phi$, where $N_\Phi = \Phi/\Phi_0$

[5] Present address: Nanoscience Center, Department of Physics, University of Jyväskylä, PO Box 35, FIN-40014, Finland.

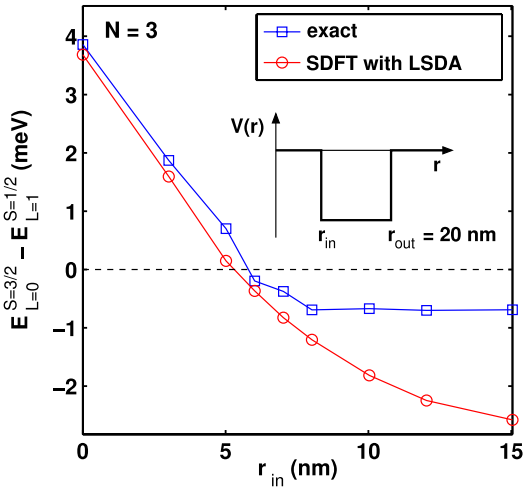

Figure 1. Total-energy differences between the states $L = 0$, $S = 1/2$ and $L = 1$, $S = 3/2$ in a three-electron quantum ring as a function of the inner radius ($r_{\rm in}$) of the ring. The outer radius is fixed to $r_{\rm out} = 20$ nm. The squares show exact-diagonalization results from [20], and the circles show our results from the local spin-density approximation within the spin-density-functional theory.

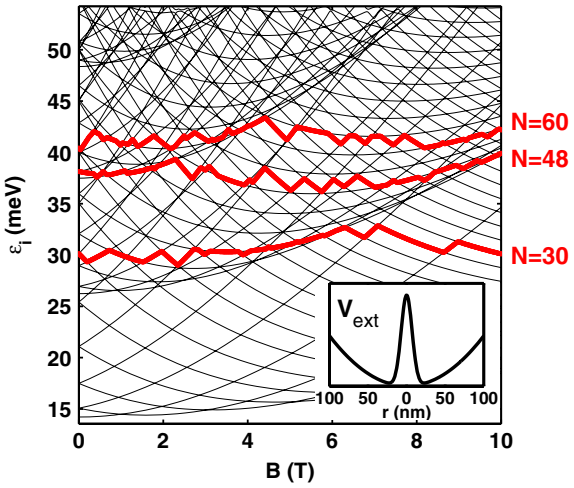

Figure 2. Single-electron spectrum of the quantum ring. The inset shows the corresponding external potential defined in equation (2). The thick red (gray) lines correspond to the electron numbers considered in this work, assuming that the states below the lines are filled and spin degenerate.

is the number of flux quanta. Yet another estimation is the concept of average filling factor introduced by Kinaret *et al* [15], $\nu_{\rm avg} = N^2/[2(N + L)]$, where L is the total angular momentum.

In this paper we study the characteristics of quantum Hall states at $\nu > 1$ in QRs up to $N = 60$. We apply efficient numerical algorithms based on spin-density-functional theory to calculate the ground-state energies and spin densities as a function of the magnetic field. We find that characteristic features in the total energies can be associated with specific integer (and half-integer) values of $\nu_{\rm LL}$. The values obtained for $\nu_{\rm avg}$ and ν_Φ differ considerably from $\nu_{\rm LL}$ in the low-field regime, although the differences decrease as a function of N. The state $\nu = 2$ can be found consistently using all three definitions. In the large-N regime, we are also able to find signatures of the fractional $\nu = 5/2$ state. Despite the different topology of QRs compared with harmonic QDs, the characteristics of this state are found to be similar: the electrons in the second-lowest Landau level form a spin-polarized droplet (spin droplet) on top of the spin-compensated lowest Landau level.

2. Model and methods

The many-electron Hamiltonian can be written as

$$H = \frac{1}{2m^*}\sum_{i=1}^{N}[-{\rm i}\hbar\nabla_i + e\mathbf{A}(\mathbf{r}_i)]^2 + \sum_{i<j}^{N}\frac{e^2}{4\pi\epsilon_0\kappa|\mathbf{r}_i - \mathbf{r}_j|} + \sum_{i=1}^{N}\left[V_{\rm ext}(r_i) + g^*\mu_{\rm B}Bs_{z,i}\right]. \quad (1)$$

where $\mathbf{B} = B\hat{z}$ is perpendicular to the 2D (xy) plane, where the electrons are restricted, thus approximating the semiconductor heterostructure. We use the effective-mass approximation for electrons in GaAs with $m^* = 0.067\ m_e$, $\kappa = 12.7$, and $g^* = -0.44$. The vector potential is applied in linear gauge, i.e., $\mathbf{A} = -By\mathbf{e}_x$. The confining potential in the xy plane approximating a QR is

$$V_{\rm ext}(r) = \tfrac{1}{2}m^*\omega_0^2 r^2 + V_0 {\rm e}^{-r^2/d^2}, \quad (2)$$

where $\hbar\omega_0 = 5$ meV is the harmonic confinement strength, and the exponential term defines the repulsive scattering center. We set $V_0 = 200$ meV and $d = 10$ nm, yielding the potential minima at $r \sim 20$ nm (see the inset of figure 2). We note that the external confinement of equation (2) is qualitatively similar to that applied by Tan and Inkson [16].

We solve the ground-state problem associated with the Hamiltonian (1) by applying spin-density-functional theory (SDFT) in the collinear-spin representation, and with the external vector potential included in the Kohn–Sham equation. For the exchange–correlation energies we use the 2D local spin-density approximation (2D-LSDA) with the parametrization for the correlation energy provided by Attaccalite *et al* [17]. In QD studies, the 2D-LSDA within SDFT has been found to yield a good accuracy compared with quantum Monte Carlo calculations up to high magnetic fields (∼10 T) [18, 19].

To justify the numerical framework, we tested our LSDA scheme against exact-diagonalization results of Usukura *et al* [20] in the case of a three-electron QR in a hard-wall potential with varying ring width. Figure 1 shows the total-energy differences between the states $L = 0, S = 1/2$ and $L = 1, S = 3/2$ as a function of the inner ring radius $r_{\rm in}$, when the outer radius is fixed to $r_{\rm out} = 20$ nm. Overall, the LSDA performs very well up to $r_{\rm in} \sim 10$ nm. If the QR is made thinner, i.e., $r_{\rm out}/r_{\rm in} < 2$, the LSDA becomes less accurate. This is due to the fact that the 2D-LSDA used here begins to break down close to the (quasi-)one-dimensional limit [21]. The breaking is analogous to that of the 3D-LSDA in the 2D

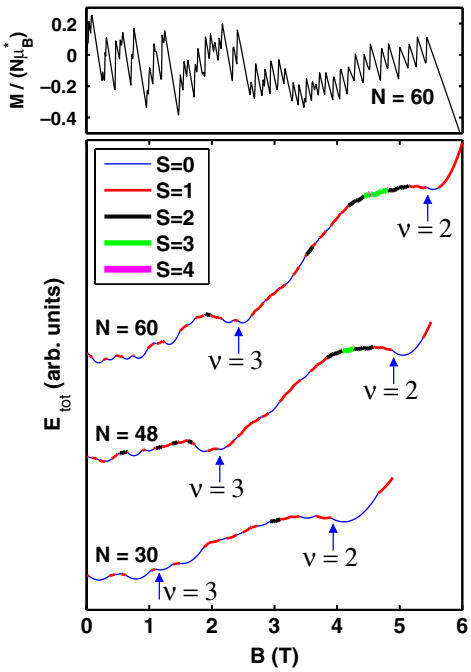

Figure 3. Upper panel: magnetization $M = -\partial E/\partial B$ of a 60-electron quantum ring as a function of the magnetic field. Lower panel: ground-state total energies E and total spins S for quantum rings with $N = 30$, 48, and 60, respectively. The arrows with numbers mark the filling factors calculated from the lowest Landau-level occupancy.

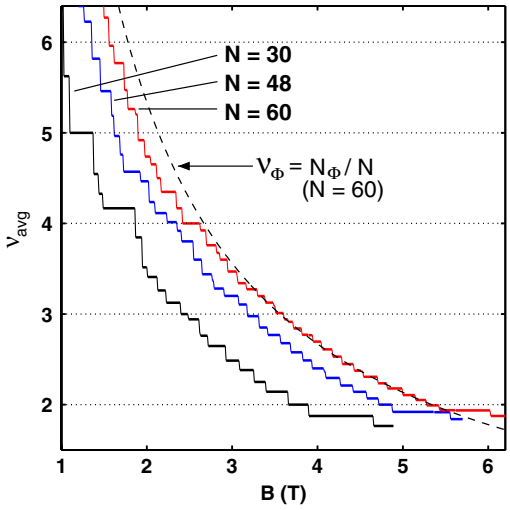

Figure 4. Average filling factors $\nu_{\rm avg}$ as a function of the magnetic field for quantum rings having 30, 48, and 60 electrons, respectively. The dashed line shows the filling factor for $N = 60$ calculated from the flux-quantum definition ν_Φ.

limit [22, 23]. It is noteworthy, however, that excluding this test case the QRs considered in this work are broadly in the 2D regime with $3 < r_{\rm out}/r_{\rm in} < 5$. More importantly, the accuracy of the LSDA is well known to increase as a function of N. Since we consider large QRs with $N \geqslant 30$ electrons, we except to encounter no problems with the reliability of 2D-LSDA within SDFT. Previous LSDA studies on finite-width QRs [8, 24], containing considerably fewer electrons than in this study, also support our numerical framework.

For the details of the numerical implementation of the SDFT method we refer to appendix 1 of [8]. Here we mention, however, that our key points to make the solution of the Kohn–Sham equations efficient are (i) applying a fourth-order factorization of the evolution operator in the eigenvalue problem and (ii) using the response-function formalism to reduce the number of self-consistency loops. These developments allow the calculation of hundreds of many-electron states for different N, B, and total spin S (z component), respectively, in a reasonable computing time.

3. Results

Figure 2 shows the single-electron spectrum of a QR defined by the confining potential in equation (2). Note that the spectrum corresponds to noninteracting electrons, i.e., the result obtained by solving the *one-electron* eigenvalue problem. Nevertheless, the spectrum gives insight into the true many-electron properties considered below. The eigenvalue spectrum has the well known periodic structure [25]. The thick red (gray) lines mark the energies corresponding to electron numbers considered in this work, assuming that the states below these lines are filled and spin degenerate in this noninteracting picture. In all these cases, single-electron states in two or three lowest Landau levels are filled at low magnetic fields.

Next we turn our analysis to the many-electron properties such as the ground-state total energies and spins obtained using the SDFT. In figure 3 we show the total energies as a function of the magnetic field for QRs containing 30, 48, and 60 electrons, respectively. The colors (line widths) correspond to different ground-state spins. The low-field regime is generally characterized by changes between $S = 0$ and 1. When $N = 48$, however, we find several ground states with $S = 2$. This is due to the high degeneracy of the single-electron states in the low-field regime, as seen in figure 2. This leads to relatively low energies of partially spin-polarized states as a result from the reduced exchange energy. At $B = 4$–5 T we are able to find ground states up to $S = 3$ and 4 for $N = 48$ and 60, respectively. These states are reminiscent of the spin-droplet states recently found from large QDs [14]. They will be analyzed in detail below (see figure 6).

We have marked in figure 3 the estimations for the corresponding filling factors at certain magnetic fields. Here we have used the expression for ν in terms of the lowest Landau-level occupancy, $\nu_{\rm LL}$. Similar to the case of QDs [10–12], the integer values for $\nu_{\rm LL}$ correspond to locally stable points in the $(B, E_{\rm tot})$ curves. These points lead to distinctive features in the magnetization shown in the upper panel of figure 3 for $N = 60$. We point out that the magnetization is qualitatively similar to that of a circular hard-wall QD [13], where the electron density is strongly localized in a ring-shaped form due to Coulomb repulsion.

We also computed the average filling factors $\nu_{\rm avg}$ (see section 1) for these systems. Figure 4 shows the results for $N = 30$, 48, and 60, respectively. Comparison to figure 3 indicates that the values for $\nu_{\rm avg}$ and $\nu_{\rm LL}$ differ

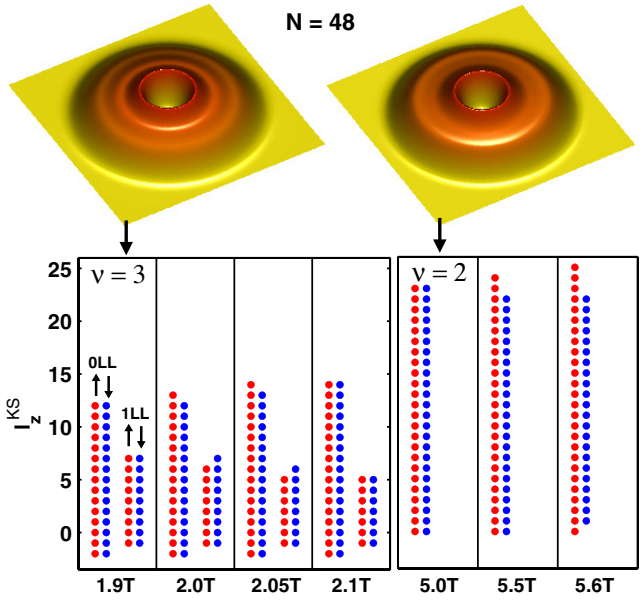

Figure 5. Upper panel: total electron densities of a 48-electron quantum ring at $B = 1.9$ and 5.0 T, respectively. Lower panel: fillings of the Kohn–Sham angular-momentum states in the lowest (0LL) and second-lowest (1LL) Landau levels at different magnetic fields. Red (light gray) and blue (black) circles correspond to spin-up and spin-down electrons, respectively.

considerably. The difference results from the fact that $\nu_{\rm avg}$ assumes a 'flat' electron density, whereas QRs are considerably inhomogeneous systems. We note, however, that as the electron number increases the difference between $\nu_{\rm LL}$ and $\nu_{\rm avg}$ becomes smaller. For example, in a 60-electron QR the values agree well for $\nu = 2$ at $B \sim 5.4$ T.

In figure 4 it is interesting to notice that in low fields $\nu_{\rm avg}$ is consistent with the conventional flux-quantum definition $\nu_\Phi = N/N_\Phi$, which is plotted for $N = 60$ (dashed line). In the calculation of ν_Φ, however, the estimation of the magnetic flux $\Phi = \pi r_0^2 B$ is cumbersome due to uncertainty in the actual ring area. The uncertainty results from the soft confining potential shown in the inset of figure 2. In this case we have fixed the point $\nu_{\rm avg} = \nu_\Phi = 2$, corresponding to the QR radius $r_0 = 86$ nm. At this radius the relative electron density is $n(r_0)/n_{\rm MAX} \sim 0.15$, so the approximation is reasonable in view of the fact that $n(r_0)/n_{\rm MAX}$ reaches ∼0.01 around $r \sim 95$ nm.

Next we analyze in detail the electron occupations of the Kohn–Sham states corresponding to $\nu_{\rm LL} = 3$ and 2. The upper panel of figure 5 shows the total electron densities of a 48-electron QR at these filling-factor values. In both cases the maximum density is peaked at the potential minima close to the 'antidot' region (see the inset of figure 2). The localization of the density in this region is enhanced by the Coulomb repulsion. The density of the $\nu_{\rm LL} = 3$ state at $B = 1.9$ T shows an additional shell compared with the relatively smooth density of the $\nu_{\rm LL} = 2$ state at 5.0 T. The shell structure accounts for the occupation of the Kohn–Sham states shown in the lower panel of figure 5. At $\nu_{\rm LL} = 3$, about one-third of the electrons are occupied in the second-lowest Landau level (1LL), yielding the local bump in the electron density. When B is increased, the electrons in the 1LL gradually jump into the 0LL, as shown in figure 5 for the first few steps at $1.9\ {\rm T} < B \leqslant 2.1$ T. Finally, the 1LL is empty of electrons and the $\nu_{\rm LL} = 2$ state is reached. In all QRs studied, we found $\nu_{\rm LL} = 2$ to be a compact state having spin-degenerate occupations $l_z^{\rm KS} = 0, 1, \ldots, N/2 - 1$ as visualized in the lower-right panel of figure 5. Further increase of the magnetic field leads to spin polarization of the 0LL. This behavior is similar to what has been found in previous theoretical studies on small ($N \leqslant 24$) QRs [8], and also experimentally in Coulomb-blockade measurements of QRs [26].

Finally, we focus on an effect of pronounced spin polarization in large QRs at magnetic fields *between* the above considered $\nu_{\rm LL} = 3$ and 2 states. The strength of the effect, i.e., the highest ground-state spin found, depends on N as seen in figure 3: for $N = 30$, 48, and 60 we find a maximum spin of $S = 2$, 3, and 4, respectively. In figure 6 we show the spin densities and electron occupations of the $S = 4$ state when $N = 60$. The spin-up density is strongly condensed near the inner edge of the QR. It accounts for the spin-polarized electrons in the 1LL. The electrons in the 0LL, on the other hand, form a relatively flat background of electrons throughout the QR area. The occupations in the right panel of figure 6 show that, at the point of maximum total spin, the 1LL is *completely* spin polarized. According to the sequence of

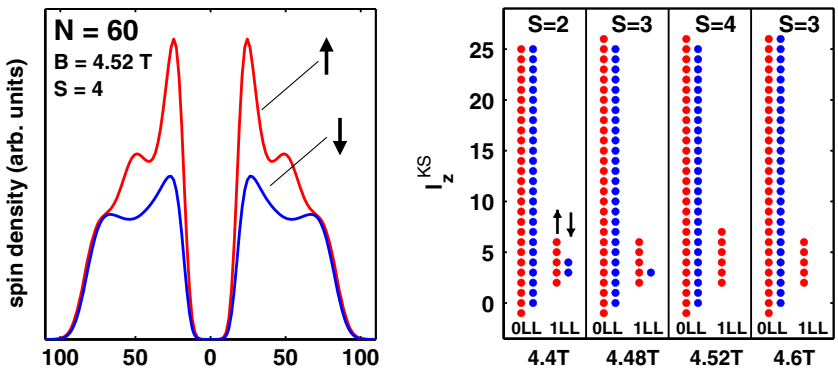

Figure 6. Left panel: spin densities of the partially spin-polarized $S = 4$ ground state in a 60-electron quantum ring. Right panel: sequence of ground states around the maximally polarized ground state ($S = 4$) at $3 > \nu > 2$. The figure shows the fillings of the Kohn–Sham angular-momentum states for spin-up (red/light gray) and spin-down (blue/dark gray) electrons on the two lowest Landau levels.

ground-state occupations around this point, the polarization occurs in magnetic fields just below the formation of the $\nu_{\rm LL} = 2$ state: for the last electrons in the 1LL, the spin-down electrons either flip their spin or jump directly into the 0LL, so that eventually the 1LL is left only with spin-up electrons. When B is increased further, the spin-up electrons jump one by one from the 1LL into the 0LL.

The characteristics of the partial spin polarization in large QRs at $3 > \nu_{\rm LL} > 2$ are very similar to what has been found in large ($N > 30$) QDs. In both systems the degeneracy of the single-electron Kohn–Sham states is very high in this regime. Therefore, the polarization can be explained by the Stoner criterion, i.e., ferromagnetic alignment due to high density of states near the Fermi level in a highly correlated system [27]. In QDs the state of maximum spin polarization of the 1LL has been interpreted as the finite-size counterpart of the fractional $\nu = 5/2$ state [13]. In contrast to the properties of uniform 2D electron gas, the $\nu = 5/2$ state in QDs has been found to have a low overlap with the corresponding Moore–Read-type Pfaffian state [28]. Furthermore, the formation of the spin-polarized many-electron state at $5/2 \geqslant \nu > 2$ in QDs, termed the 'spin-droplet state', has been indirectly confirmed in experiments [14]. The formation of such a spin-droplet state in QDs could explain the observed instabilities of the $\nu = 5/2$ state in the vicinity of quantum point contacts (QPCs) [29]: the breakdown of the bulk $\nu = 5/2$ state could be similar in restricted geometries such as in QPCs, QDs, or QRs. In this respect, our results for QRs confirm the high stability of the spin-droplet state: the spin-polarized regime in the system remains despite the deformation of a QD topology into a QR one. An important point here is the difference from the uniform 2D electron gas, where the electron pairing makes the $\nu = 5/2$ quantum Hall state appealing for quantum computations due to non-Abelian braiding statistics [30]. So far there is no evidence of this effect in confined systems.

4. Summary

To summarize, we have studied the electronic properties of relatively large ($30 \leqslant N \leqslant 60$) quantum rings in magnetic fields. We have compared different estimations for the filling factors and found that proportions in the Landau-level occupations provide a consistent definition of integer filling-factor states in quantum rings. We have found that the $\nu = 2$ state forms through partially spin-polarized states, and the magnitude of the polarization strongly depends on the number of electrons in the ring. Despite the different topology of the system, this feature is very similar to the spin-droplet state found in semiconductor quantum dots at $5/2 \geqslant \nu > 2$.

Acknowledgments

We thank E Krotscheck, S A Chin, S Janecek, R J Haug, H Saarikoski, and A Harju for useful discussions. This study was supported by the EU's Sixth Framework Program through the Nanoquanta NoE (NMP4-CT-2004-500198), Austrian Science Fund FWF under grant No. P18134, the Academy of Finland. Generous computational support was provided by the Central Computing Services at the Johannes Kepler Universität Linz.

References

[1] Lorke A, Luyken R J, Govorov A O, Kotthaus J P, Garcia J M and Petroff P M 2000 *Phys. Rev. Lett.* **84** 2223
[2] Fuhrer A, Lüscher S, Ihn T, Heinzel T, Ensslin K, Wegscheider W and Bichler M 2001 *Nature* **413** 822
[3] Keyser U F, Fühner C, Borck S, Haug R J, Bichler M, Abstreiter G and Wegscheider W 2003 *Phys. Rev. Lett.* **90** 196601
[4] Räsänen E, Castro A, Werschnik J, Rubio A and Gross E K U 2007 *Phys. Rev. Lett.* **98** 157404
[5] Niemelä K, Pietiläinen P, Hyvönen P and Chakraborty T 1996 *Europhys. Lett.* **36** 533
[6] Deo P S, Koskinen P, Koskinen M and Manninen M 2003 *Europhys. Lett.* **63** 846
[7] Emperador A, Pederiva F and Lipparini E 2003 *Phys. Rev.* B **68** 115312
[8] Aichinger M, Chin S A, Krotscheck E and Räsänen E 2006 *Phys. Rev.* B **73** 195310
[9] Keyser U F, Fühner C, Borck S, Haug R J, Wegscheider W and Bichler M 2003 *Adv. Solid State Phys.* **43** 113
[10] For a review, see, e.g. Kouwenhoven L P, Austing D G and Tarucha S 2001 *Rep. Prog. Phys.* **64** 701
Reimann S M and Manninen M 2002 *Rev. Mod. Phys.* **74** 1283
[11] Oosterkamp T H, Janssen J W, Kouwenhoven L P, Austing D G, Honda T and Tarucha S 1999 *Phys. Rev. Lett.* **82** 2931
[12] Ciorga M, Sachrajda A S, Hawrylak P, Gould C, Zawadzki P, Jullian S, Feng Y and Wasilewski Z 2000 *Phys. Rev.* B **61** R16315
[13] Harju A, Saarikoski H and Räsänen E 2006 *Phys. Rev. Lett.* **96** 126805
[14] Räsänen E, Saarikoski H, Harju A, Ciorga M and Sachrajda A S 2008 *Phys. Rev.* B **77** 041302(R)
[15] Kinaret J M, Meir Y, Wingreen N S, Lee P A and Wen X G 1992 *Phys. Rev.* B **46** 4681
[16] Tan W-C and Inkson J 1996 *Semicond. Sci. Technol.* **11** 1635
[17] Attaccalite C, Moroni S, Gori-Giorgi P and Bachelet G B 2002 *Phys. Rev. Lett.* **88** 256601
[18] Saarikoski H, Räsänen E, Siljamäki S, Harju A, Puska M J and Nieminen R M 2003 *Phys. Rev.* B **67** 205327
[19] Helbig N, Kurth S, Pittalis S, Räsänen E and Gross E K U 2008 *Phys. Rev.* B **77** 245106
[20] Usukura J, Saiga Y and Hirashima D S 2005 *J. Phys. Soc. Japan* **74** 1231
[21] Räsänen E, Pittalis S, Proetto C R and Gross E K U 2008 submitted (arXiv:0807.1868)
[22] Kim Y-H, Lee I-H, Nagaraja S, Leburton J-P, Hood R Q and Martin R M 2000 *Phys. Rev.* B **61** 5202
[23] Pollack L and Perdew J P 2000 *J. Phys.: Condens. Matter* **12** 1239
[24] Emperador A, Pi M, Barranco M and Lipparini E 2001 *Phys. Rev.* B **64** 155304
[25] See, e.g. Simonin J, Proetto C R, Barticevic Z and Fuster G 2004 *Phys. Rev.* B **70** 205305 and references therein
[26] Keyser U F 2002 *PhD Thesis* University of Hannover
[27] Stoner E C 1938 *Proc. R. Soc.* A **165** 372
[28] Moore G and Read N 1991 *Nucl. Phys.* B **360** 362
[29] Miller J B, Radu I P, Zumbuhl D M, Levenson-Falk E M, Kastner M A, Marcus C M, Pfeiffer L N and West K W 2007 *Nat. Phys.* **3** 561
[30] Das Sarma S, Freedman M and Nayak C 2005 *Phys. Rev. Lett.* **94** 166802
For a recent review, see also Das Sarma S, Freedman M, Nayak C, Simon S H and Stern A 2007 arXiv:070.1889